ISCI, Volume *17*

Supplemental Information

Membrane-Deformation Ability of ANKHD1 Is Involved in the Early Endosome Enlargement

Manabu Kitamata, Kyoko Hanawa-Suetsugu, Kohei Maruyama, and Shiro Suetsugu

Transparent Methods

Antibodies

The following antibodies were used: rabbit anti-GFP antibody (MBL Life Science, 598), rabbit anti-ANKHD1 antibody (Atlas Antibodies, HPA008718), mouse anti-EEA1 antibody (BD Biosciences, 610456), rabbit anti-EEA1 (Cell Signaling Technology, 3288), mouse anti-GAPDH antibody (Santa Cruz Biotechnology, sc-166574), mouse anti-GM130 antibody (BD Biosciences, 610822), mouse anti-Bcl-2 antibody (BD Biosciences, 610538), mouse anti-Calnexin antibody (Santa Cruz Biotechnology, sc-23954), mouse anti-mCherry antibody (Novus, NBP1-96752), mouse anti-Rab5 antibody (Santa Cruz Biotechnology, sc-46692), mouse anti-LAMP1 antibody (Santa Cruz Biotechnology, sc-20011), and mouse anti-Tom20 antibody (Santa Cruz Biotechnology, sc-17764).

Plasmids

Glutathione S-transferase (GST)-tagged human ANKHD1 fragments of 195–1418 aa (ARD25) were amplified by PCR using the following primers: 5’-GAAGATCTGCAGAAAACAGCCACAATG-3’ and 5’-GAAGATCTTTAGTCTTTAGCCTTCACAATG-3’. They were then inserted into the pCold vector (TaKaRa Bio) at the BamH1 restriction site.

To prepare the pVenus×3 vector, EGFP in the pEGFP-N3 vector was replaced with Venus×3. The vector backbone of the pEGFP-N3 vector was amplified by the following primers: 5’-TAAAGCGGCCGCGACTCTAG-3' and 5’-GGTGGCGATGGATCCCGGG-3’. Each Venus cDNA was amplified by the following primers:

5’-CCGGGATCCATCGCCACCATGGTGAGCAAGGGCGAG-3’ and 5’-GGCAGATCTGAGTCCGGACTTGTACAGCTCGTCCATG -3’.

5’- TCCGGACTCAGATCTGCCACCGCGGTGAGCAAGGGCGAGGAG-3’ and 5’-CGCGGTGGCGATGGATCCGCTCTTGTACAGCTCGTCCATGC-3’.

5’-GCGGATCCATCGCCACCGCGGTGAGCAAGGGCGAGGAGC-3’ and 5’-CTAGAGTCGCGGCCGCTTTACTTGTACAGCTCGTCCATGC-3’.

These four fragments were assembled using the Gibson Assembly Master Mix (New England BioLabs).

The pVenus×3-ANKHD1 plasmid was prepared by assembly using Gibson Assembly Master Mix. The five cDNA fragments included cDNA of full-length ANKHD1, three Venus cDNAs, and the backbone of pEGFP-N3 vector. The backbone of pEGFP-N3 vector was amplified by PCR with the primers: 5'-TAAAGCGGCCGCGACTCTAG-3' and 5'-ATCAGTCAGCATGGTGGCAGATCTGAGTCCGGTAGCGC-3'.

The three Venus sequences were amplified by PCR with the following primers: 5'-TCTCAAATATGTCAACAGCGGATCCATCGCCACCGCGGTGAGCAAGGGCG-3' and 5'-GGCAGATCTGAGTCCGGACTTGTACAGCTCGTCCATG-3', 5'-TCCGGACTCAGATCTGCCACCGCGGTGAGCAAGGGCGAGGAG-3' and 5'-CGCGGTGGCGATGGATCCGCTCTTGTACAGCTCGTCCATGC-3', 5'-AGCGGATCCATCGCCACCGCGGTGAGCAAGGGCGAGGAGC-3' and 5'-CTAGAGTCGCGGCCGCTTTACTTGTACAGCTCGTCCATGC-3'.

The ANKHD1 cDNA was amplified by PCR with the following primers: 5'-GAAGATCTGCCACCATGCTGACTGATAGCGGAGG and GAAGATCTGTTGACATATTTGAGATGC-3'. The amplified cDNA sequence was inserted into the pMD20-T vector using Mighty TA-cloning Kit (TaKaRa Bio) and then extracted by BglII digestion.

To prepare the siRNA resistant constructions of ANKHD1, five silent mutations were induced in each target sequence of three siRNAs: 5′-GGTGGAAACAGCGACTCTGATAAC-3′, 5′-GTGACACCCAACTCTTTGTCCACCAG-3′, and 5′-AGCAGCTGTGCGTGACAAACACCCGG-3′.

Protein purification

Plasmids for expression of GST-fused protein were transformed into Rosetta2 cells (Novagen). The cells were cultured in Luria broth (LB) medium at 37°C, and the proteins were overexpressed using 1 mM isopropyl β-D-1-thiogalactopyranoside overnight at 12°C. The cells were collected and then lysed in a buffer containing 10 mM Tris-HCl (pH 7.5), 150 mM NaCl, 1 mM EDTA, 0.5% Triton X-100 (8 mM), 2 mM 2-mercaptoethanol, and 1 mM phenylmethylsulfonyl fluoride using an ultrasonic

homogenizer. The lysate was centrifuged and the supernatant was incubated with the glutathione-sepharose 4B beads. The beads were washed four times using approximately 10-fold dilutions in 10 mM Tris-HCl (pH 7.5), 150 mM NaCl, 1 mM EDTA, and 1 mM dithiothreitol (DTT), and protein was collected by cleavage from the GST tag by precision protease at 4°C overnight.

Preparation of liposomes

PC (Sigma-Aldrich, P3841), PE (Sigma-Aldrich, P7693), PS (Sigma-Aldrich P5660), and porcine brain Folch fractions (Avanti) were dissolved in chloroform and mixed using defined weigh ratios to 0.2 mg/ml concentration of total lipid. Rhodamine-PE (Avanti, 810150) was incorporated at 0.2%. The lipids were dried under nitrogen gas and subsequently maintained under vacuum for 20 min to remove residual chloroform. The dried lipids were suspended in buffer containing 10 mM Tris-HCl (pH 7.5), 150 mM NaCl, and 1 mM EDTA and then incubated for 1 hr at 37°C. In Figure S10, liposomes were extruded 11 times with 800 nm polycarbonate filters using an extruder (Avanti).

Liposome sedimentation assay

The protein aggregates were removed by ultracentrifugation before incubation with liposomes. The prepared liposomes (0.2 mg/ml) were incubated with the proteins in buffer containing 10 mM Tris-HCL (pH 7.5), 150 mM NaCl, 1 mM EDTA, and 0.5 mM DTT for 30 min at room temperature. After incubation, these reaction solutions were centrifuged at 109000 × g for 20 min to examine the vesiculation and at 245000× g for 20 min to examine the membrane binding at room temperature in a TLA-100 rotor (Beckman). The supernatant and the pellet fractions were separated, and SDS-PAGE sample buffer was added into these fractions to the same volume, and then analyzed by SDS-PAGE. The fluorescence of rhodamine-PE was measured using an FLA-8000 fluorescence image analyzer (Fuji-Film). The band intensities were quantified by ImageJ software.

Electron microscopy

Proteins were incubated with liposomes (0.2 mg/ml) prepared as described above in a

buffer containing 10 mM Tris-HCl (pH 7.5), 150 mM NaCl, and 1 mM EDTA. After incubation for 20 min at 25°C, a formvar-coated grid was put on the reaction mixture, washed with 100 mM HEPES (pH 7.5), and then stained with 0.5% uranyl acetate for 30 s. The grid was observed by transmission electron micrography using a model H-7100 microscope (Hitachi).

Crosslinking analysis

Proteins were incubated with or without liposomes (0.2 mg/ml) in buffer containing 10 mM HEPES (pH 8.0), 150 mM NaCl, 1 mM EDTA, and 0.5 mM DTT for 30 min at room temperature. The mix solution was incubated with BS(PEG)5 (Thermo Fisher Scientific, 21581) for 30 min at room temperature. The reaction was quenched by adding SDS-PAGE sample buffer and then analyzed by SDS-PAGE.

Transfection and siRNA treatment

HeLa, HEK293T, Caki-1, U2OS, and DLD1 cells were cultured in Dulbecco's modified Eagle's medium containing 10% fetal bovine serum with penicillin and streptomycin at 37°C in an atmosphere of 5% CO_2. One day before transfection, 5×10^4 cells were seeded in wells of 6-well dishes. The cells were transfected using Lipofectamine 3000 (Invitrogen). After 24 hr of transfection, the cells were analyzed.

Knockdown of ANKHD1 was performed with stealth RNAi (Invitrogen). The siRNA sequences were 5'-CAGGUGGGAAUAGUGAUUCAGAUAA-3', 5'-GAAGUGACUCCUAAUUCCUUGUCAA-3', and 5'-CAGUCAGCAACUGUGUGUCACUAAU-3'. These siRNAs were mixed and transfected using Lipofectamine 3000. The stealth RNAi siRNA Negative Control (Invitrogen) was also transfected as a control. One day before transfection of siRNA, 5×10^4 cells were seeded in wells of 6-well dishes, and then siRNA was transfected into the cells. After 48 hr of transfection, the cells were analyzed.

Immunostaining

HeLa cells were fixed in 4% paraformaldehyde for 10 min, permeabilized in a buffer containing 0.1% Triton X-100, 50 mM Tris-HCl (pH 7.5), and 100 mM NaCl for 10 min, and then blocked in 1% bovine serum albumin, 50 mM Tris-HCl (pH 7.5), and 100

mM NaCl for 1 hr. The cells were incubated with primary antibody in buffer containing 1% BSA, 50 mM Tris-HCl (pH 7.5), and 100 mM NaCl for 1 hr. After washing with PBS, the cells were incubated with secondary antibodies conjugated with Alexa Fluor 488 and 568 in buffer containing 1% BSA, 50 mM Tris-HCl (pH 7.5), and 100 mM NaCl for 1 hr. The cells were washed using PBS and mounted in ProLong Diamond Antifade Mountant (Invitrogen).

All fluorescence images were acquired by confocal microscopy (FV1000D, Olympus). A 100× immersion objective lens (NA 1.40, Olympus) was used for live cell and fixed cell imaging. Z-stack images were captured at 0.4 μm intervals.

Live cell imaging

Mitochondria were stained with 200 nM Mitotracker Red CM-H_2Xros (Molecular Probes, M7513) at 37°C in an atmosphere of 5% CO_2 for 45 min. Lysosomes were stained using 75 nM Lysotracker Red DND-99 (Molecular Probes, L7528) at 37°C in an atmosphere of 5% CO_2 for 1 hr. Live cells were observed by confocal microscopy at 37°C in the 5% CO_2 atmosphere.

Quantification of organelle area

The number of puncta, average area, and total area of organelles per cell were calculated from images with the focal plane in the vicinity of coverslips, where the area of the cell is the largest, using ImageJ software. Images of the organelles were converted into binary images and set in equal thresholds in each experiment. Then, the minimal particles size was set to 0.04 μm^2 and evaluated by the *Analyze Particles* function in the ImageJ software.

Quantification of colocalization in cells

The percentages of colocalization per cell in Figure 3, Figure S6, and Figure S7 were calculated using the *Colocalization Threshold* function in the ImageJ software. Colocalization represented the overlap with green and red channel intensities above a threshold and indicates the pixels that have both channels. The percentages of colocalization were calculated as the number of pixels that had both channels / total number of pixels of each channel. Fluorescence images were set in equal thresholds in

each experiment.

Statistical analysis

Statistical differences were analyzed using paired two tailed Student's *t*-test in Figure 1, Figure 2B, Figure 5, Figure 6, Figure 7B, Figure S4, Figure S6B and Figure S10. Unpaired two tailed Student's *t*-test were performed in Figures 2D-2E, Figures 2G-2H, Figure 2J, Figure 2L, Figure 3, Figure 4, Figures 7D-7F, Figure 8, Figure S5, Figures S6D-S6H, Figure S8, and Figure S9. *P*-values and the number of repeated experiments are described in the figures and figure legends. All error bars represent standard error.

Supplemental Figure Legends.

Figure S1. Domain structure of 18 ARDs containing fragments and these EST frequencies, Related to Figure 1.

(A) Illustration of the ankyrin repeat proteins. The 18 ARD fragments, surrounded by red lines, were used in Figure 1.

(B) Average EST frequencies (TPM: Transcripts per million) of 18 ARDs containing fragments among 78 organs/health states/developmental stages in the Unigene database (https://www.ncbi.nlm.nih.gov/unigene).

Figure S2. Phylogenetic tree of ankyrin repeats from human 18 ARD proteins, Related to Figure 1.

Phylogenetic tree of ankyrin repeats from human 18 ARD proteins is shown. The amino acid sequences of the ankyrin repeats within each protein are compared in the highly transcribed human 18 ARD proteins (Figure S1). Red and blue indicate ANKHD1 and ANKRD17, respectively.

Figure S3. Phylogenetic tree of ankyrin repeats from all human proteins, Related to Figure 1.

Phylogenetic tree of ankyrin repeats of all human proteins from SMART (http://smart.embl-heidelberg.de) is shown. The amino acid sequences of ankyrin repeats within each protein are compared in all human proteins. Red indicates ANKHD1. The names of proteins other than ANKHD1 are not shown.

Figure S4. Localization of ANKHD1 on EEA1-positive early endosomes in HEK293T, Caki-1, U2OS, and DLD1 and increased EEA1-positive early endosomes in ANKHD1-depleted cells, Related to Figure 2 and Figure 3.

(A) Effects of ANKHD1 knockdown on the levels of endogenous EEA1 in HEK293T, Caki-1, U2OS, and DLD1 cells treated with control or ANKHD1 siRNA. The whole-cell lysates were subjected to western blotting with anti-EEA1 antibody. GAPDH was examined as the loading control. Data represent the mean of four independent experiments. Error bars represent SE. $*P < 0.05$ and $**P < 0.01$. Statistical significance

was determined with the Student's *t*-test.
(B) Confocal microscopy images of endogenous ANKHD1 (green) and EEA1 (red) in HEK293T, Caki-1, U2OS, and DLD1 cells. Arrows indicate colocalization of endogenous ANKHD1 and EEA1. Scale bars, 10 μm. Scale bars in magnification, 2 μm.

Figure S5. The total area and number of EEA1-positive early endosomes at each focal plane in HeLa cells, Related to Figure 2.
(A) The z-stack images of EEA1 in HeLa cells. The lower panel shows the z section at the yellow line at the upper panel. The z-stack images were taken at 0.4 μm intervals for the measurement of EEA1 puncta in each focal plane. At the lower panel, the z axis was enlarged five times.
(B-C) The total area (B) and the number (C) of EEA1 puncta per cell in each focal plane were measured by ImageJ software. Confocal slices were taken at 0.4 μm intervals. Data represent the mean of 14 cells. All error bars represent SE. $*P < 0.05$, $**P < 0.01$, and $***P < 0.001$. Statistical significance was determined with the Student's *t*-test.

Figure S6. Knockdown of ANKHD1 increases the size of Rab5-positive organelles and the co-localization of Rab5 with EEA1, Related to Figure 2.
(A) Amounts of endogenous Rab5 in HeLa cells treated with control or ANKHD1 siRNA by western blotting.
(B) Quantification of Rab5 in (A). Data represent the mean of five independent experiments.
(C) Confocal microscopy analysis of endogenous Rab5 in HeLa cells treated with control or ANKHD1 siRNA by immunostaining.
(D-G) The total area (D), the number (E), the size distribution (F), and the average area (G) of Rab5 puncta per cell in (C) were measured by ImageJ software. Data represent the mean of 30 cells from three independent experiments for control siRNA and ANKHD1 siRNA.
(H) Colocalization percentages of endogenous Rab5 with endogenous EEA1 in ANKHD1-depleted cells. Date represent the mean of 7 and 8 cells for control siRNA and ANKHD1 siRNA, respectively.
All error bars represent SE. $*P < 0.05$, $**P < 0.01$, and $***P < 0.001$. Statistical

significance was determined with the Student's *t*-test. ns, not significant. Scale bars, 10 μm. Scale bars in magnification, 2 μm

Figure S7. Localization of ANKHD1 in various organelles, Related to Figure 3.

(A) Confocal microscopy images of endogenous ANKHD1 (green) and Rab5 (red) in HeLa cells. The rectangle in the upper image shows the region of enlargement in the lower images.

(B) Confocal microscopy images of endogenous ANKHD1 (green) and LAMP1 (red) in HeLa cells.

(C) Confocal microscopy images of endogenous ANKHD1 (green) and GM130 (red) in HeLa cells.

(D) Confocal microscopy images of endogenous ANKHD1 (green) and Calnexin (red) in HeLa cells.

(E) Confocal microscopy images of endogenous ANKHD1 (green) and Tom20 (red) in HeLa cells.

(F) Colocalization percentages of endogenous ANKHD1 with Rab5, LAMP1, GM130, Calnexin, or Tom20 per cell in (A-E) calculated using ImageJ software. Data represent the means of 10 (A), 10 (B), 13 (C), 15 (D), and 12 (E) cells. Error bars represent SE. Scale bars, 10 μm. Scale bars in magnification, 2 μm.

Figure S8. Knockdown of ANKHD1 does not affect maturation of early endosomes to lysosomes, Related to Figure 2.

(A) Lysosome morphology stained with Lysotracker was observed in HeLa cells treated with control or ANKHD1 siRNA.

(B-D) Quantification of (B) the number, (C) the average area, and (D) the total area of lysosomes per cell in (A). Data represent the means of 26 and 25 cells from three independent experiments for control siRNA and ANKHD1 siRNA, respectively.

All error bars represent SE. Statistical significance was determined with the Student's *t*-test. ns, not significant. Scale bars, 10 μm.

Figure S9. Effect of ANKHD1 fragments on the total area of organelles, Related to Figure 5.

(A) Amounts of expressed ANKHD1 fragments in HeLa cells expressing EGFP, N+ARD15-EGFP, ARD10-EGFP, N+ARD25-EGFP, ARD25-EGFP, or ANKHD1-EGFP by western blotting.
(B) Confocal microscopy images of expressed ANKHD1 fragments and endogenous EEA1 in HeLa cells expressing EGFP, N+ARD15-EGFP, N+ARD25-EGFP, ARD25-EGFP, or ANKHD1-EGFP.
(C-D) The total area (C) and the number (D) of EEA1 puncta per cell in (B) was measured using ImageJ software. Data represent the mean of 25, 26, 25, 24, and 26 cells from three independent experiments for EGFP, N+ARD15-EGFP, N+ARD25-EGFP, ARD25-EGFP, and ANKHD1-EGFP, respectively.
(E) Confocal microscopy analysis of endogenous Calnexin in HeLa cells expressing EGFP or N+ARD25-EGFP.
(F) The total area of Calnexin staining per cell in (E) was measured as in (C). Data represent the mean of 22 cells from three independent experiments for EGFP and N+ARD25-EGFP.
(G) Confocal microscopy analysis of mitochondria stained with Mitotracker in HeLa cells expressing EGFP or N+ARD25-EGFP.
(H) The total area of Mitotracker staining per cell in (G) was measured as in (C). Data represent the mean of 22 and 21 cells from three independent experiments for EGFP and N+ARD25-EGFP, respectively.
(I) Confocal microscopy analysis of endogenous GM130 in HeLa cells expressing EGFP or N+ARD25-EGFP.
(J-K) The total area (J) of GM130 staining measured as in (C) and the number of Golgi fragments (K) per cell in (I) are shown. Data represent the mean of 22 cells from three independent experiments for EGFP and N+ARD25-EGFP.
All error bars represent SE. $*P < 0.05$ and $**P < 0.01$. Statistical significance was determined using the Student's *t*-test. ns, not significant. Scale bars, 10 μm

Figure S10. Vesiculation ability of ANKHD1 in filtered liposome and unfiltered liposome is not different, Related to Figure 6.
(A) Vesiculation by liposome sedimentation assay for N+ARD25 with liposomes extruded through a filter of 800 nm and liposomes without extrusion. Protein

concentration is 50 nM, 150 nM, or 300 nM. The lipid composition of the liposomes was PC : PE : PS : rhodamine-PE at a weight ratio of 4 : 3 : 3 : 0.02.
(B) Quantification of liposomes in (A). The percentage of Rhodamine-PE fluorescence in the supernatant is shown. Data represent the mean of three independent experiments. Error bars represent SE. Statistical significance was determined using the Student's *t*-test. ns, not significant.

Figure S11. Structural characteristics of the latter 10 ankyrin repeats of ANKHD1, Related to Figure 6.

(A) Sequence alignment of ankyrin repeats in ANKHD1 by Clustal X. The colors are based in the Clustal X program. Red circles indicate arginine and lysine at position 1 and position 2 in ANKs.
(B) Structural model of the latter 10 ankyrin repeats (1054-1390 aa) predicted by Phyre2 (http://www.sbg.bio.ic.ac.uk/phyre2).
(C) Surface electrostatistics map of the latter 10 ankyrin repeats (1054-1390 aa) generated by Pymol using the model in (B). The amphipathic helix is also illustrated. The mutated amino acid residues, K1323, K1324, R1357, and K1358, are indicated.
(D) The hydrophobic moment of ANKHD1 calculated using Heliquest. The high score means that the helix is predicted to be an amphipathic helix. Arrow shows the highest hydrophobic moment of 1400-1415 aa in ANKHD1.
(E) The schematic illustration of the membrane deformation by the dimeric ANKHD1.

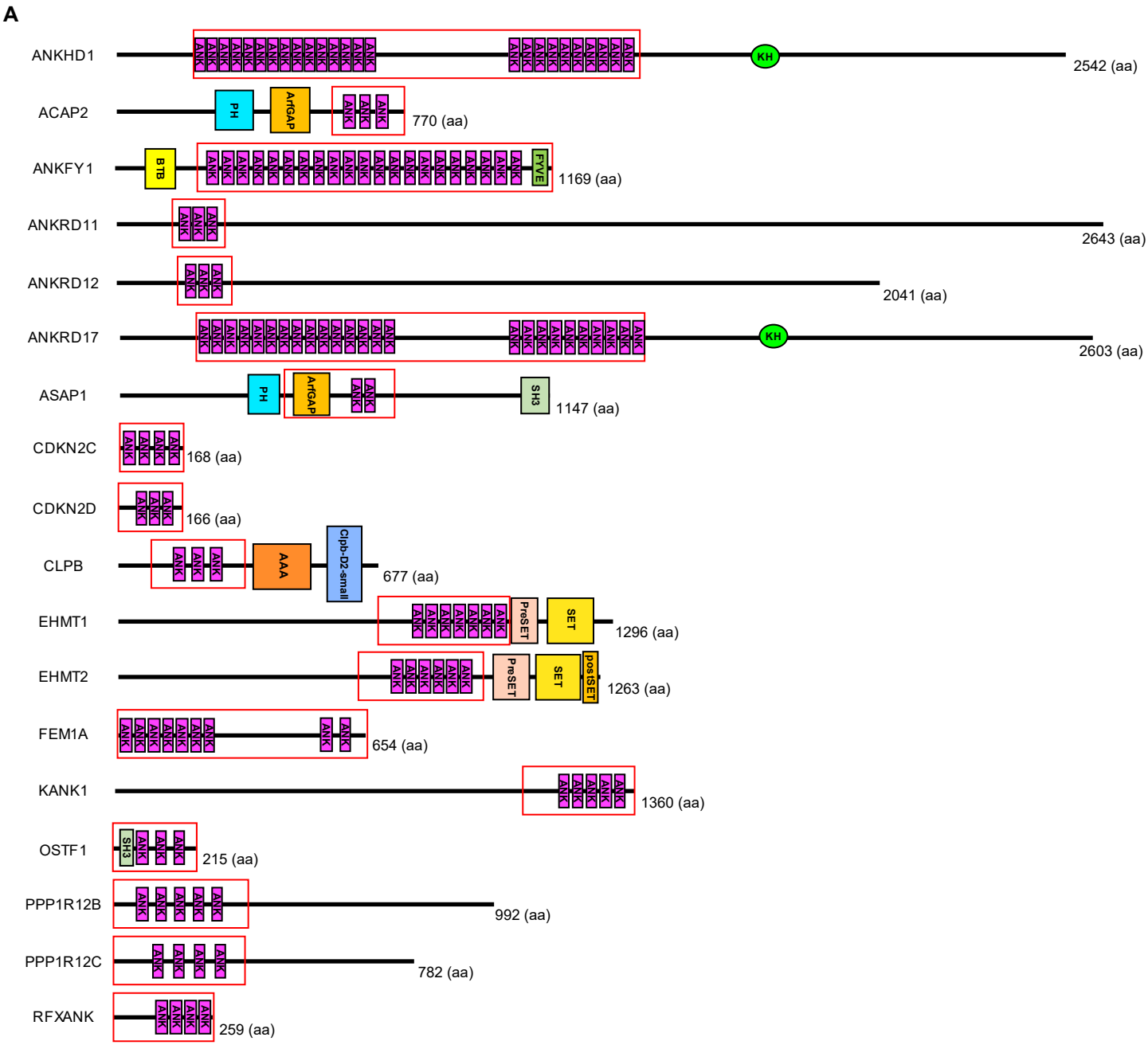
A
ANKHD1
2542 (aa)
ACAP2
770 (aa)
ANKFY1
1169 (aa)
ANKRD11
2643 (aa)
ANKRD12
2041 (aa)
ANKRD17
2603 (aa)
ASAP1
1147 (aa)
CDKN2C
168 (aa)
CDKN2D
166 (aa)
CLPB
677 (aa)
EHMT1
1296 (aa)
EHMT2
1263 (aa)
FEM1A
654 (aa)
KANK1
1360 (aa)
OSTF1
215 (aa)
PPP1R12B
992 (aa)
PPP1R12C
782 (aa)
RFXANK
259 (aa)
ANK
PH
ArfGAP
BTB
FYVE
KH
SH3
AAA
Clpb-D2-small
PreSET
SET
postSET

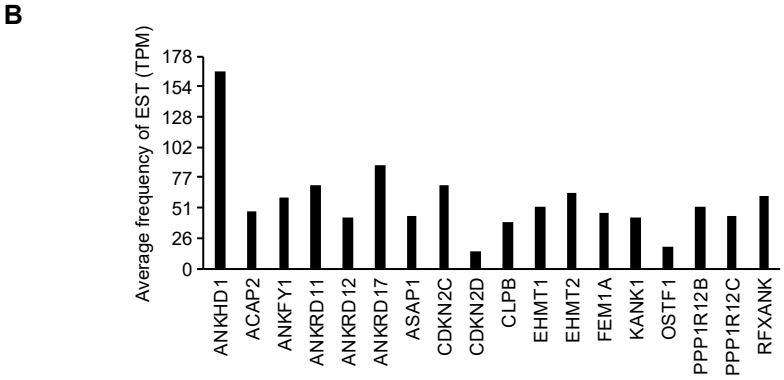
B
Average frequency of EST (TPM)
178
154
128
102
77
51
26
0
ANKHD1
ACAP2
ANKFY1
ANKRD11
ANKRD12
ANKRD17
ASAP1
CDKN2C
CDKN2D
CLPB
EHMT1
EHMT2
FEM1A
KANK1
OSTF1
PPP1R12B
PPP1R12C
RFXANK

Figure S1

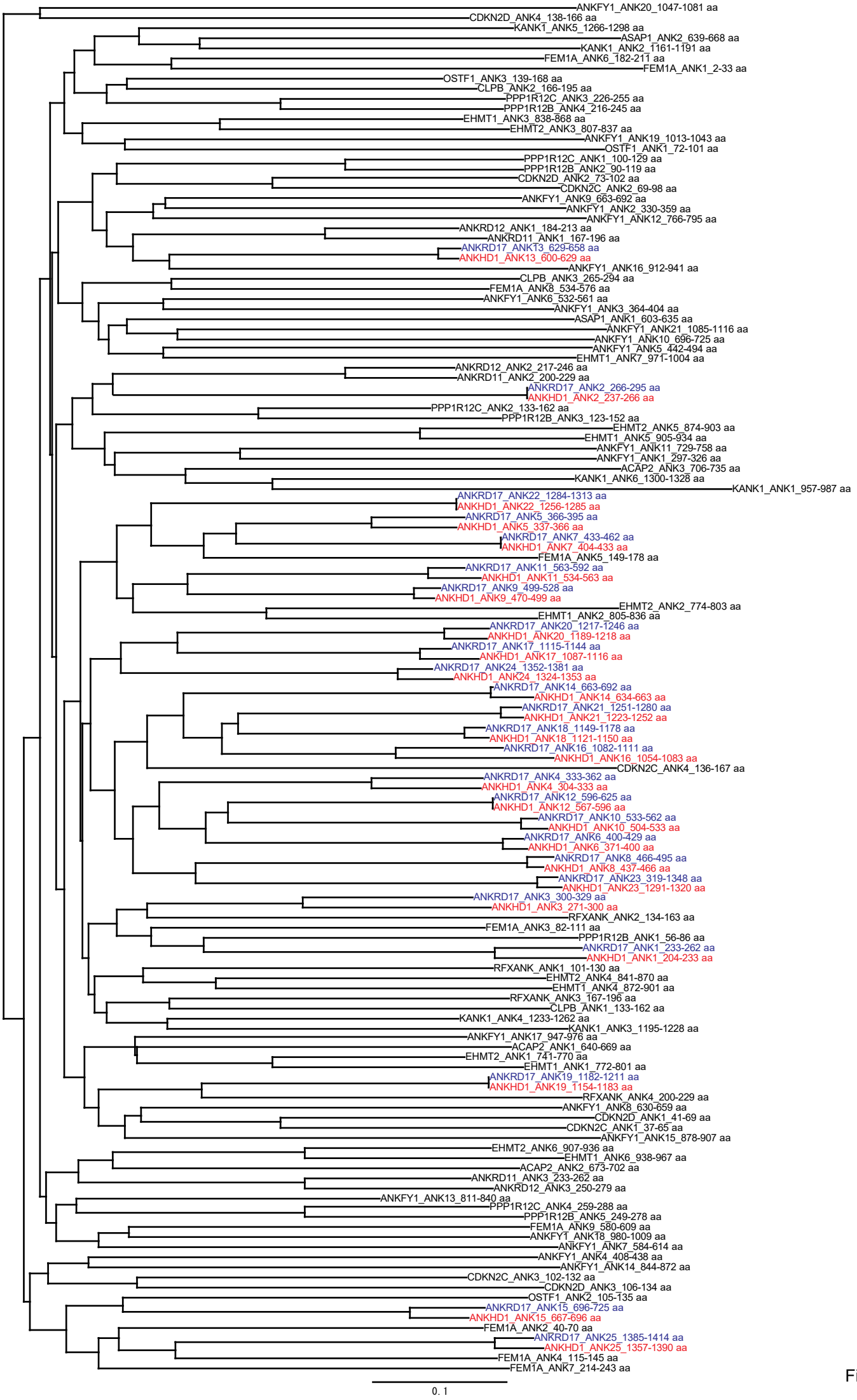
ANKFY1_ANK20_1047-1081 aa
CDKN2D_ANK4_138-166 aa
KANK1_ANK5_1266-1298 aa
ASAP1_ANK2_639-668 aa
KANK1_ANK2_1161-1191 aa
FEM1A_ANK6_182-211 aa
FEM1A_ANK1_2-33 aa
OSTF1_ANK3_139-168 aa
CLPB_ANK2_166-195 aa
PPP1R12C_ANK3_226-255 aa
PPP1R12B_ANK4_216-245 aa
EHMT1_ANK3_838-868 aa
EHMT2_ANK3_807-837 aa
ANKFY1_ANK19_1013-1043 aa
OSTF1_ANK1_72-101 aa
PPP1R12C_ANK1_100-129 aa
PPP1R12B_ANK2_90-119 aa
CDKN2D_ANK2_73-102 aa
CDKN2C_ANK2_69-98 aa
ANKFY1_ANK9_663-692 aa
ANKFY1_ANK2_330-359 aa
ANKFY1_ANK12_766-795 aa
ANKRD12_ANK1_184-213 aa
ANKRD11_ANK1_167-196 aa
ANKRD17_ANK3_629-658 aa
ANKHD1_ANK13_600-629 aa
ANKFY1_ANK16_912-941 aa
CLPB_ANK3_265-294 aa
FEM1A_ANK8_534-576 aa
ANKFY1_ANK6_532-561 aa
ANKFY1_ANK3_364-404 aa
ASAP1_ANK1_603-635 aa
ANKFY1_ANK21_1085-1116 aa
ANKFY1_ANK10_696-725 aa
ANKFY1_ANK5_442-494 aa
EHMT1_ANK7_971-1004 aa
ANKRD12_ANK2_217-246 aa
ANKRD11_ANK2_200-229 aa
ANKRD17_ANK2_266-295 aa
ANKHD1_ANK2_237-266 aa
PPP1R12C_ANK2_133-162 aa
PPP1R12B_ANK3_123-152 aa
EHMT2_ANK5_874-903 aa
EHMT1_ANK5_905-934 aa
ANKFY1_ANK11_729-758 aa
ANKFY1_ANK1_297-326 aa
ACAP2_ANK3_706-735 aa
KANK1_ANK6_1300-1328 aa
KANK1_ANK1_957-987 aa
ANKRD17_ANK22_1284-1313 aa
ANKHD1_ANK22_1256-1285 aa
ANKRD17_ANK5_366-395 aa
ANKHD1_ANK5_337-366 aa
ANKRD17_ANK7_433-462 aa
ANKHD1_ANK7_404-433 aa
FEM1A_ANK5_149-178 aa
ANKRD17_ANK11_563-592 aa
ANKHD1_ANK11_534-563 aa
ANKRD17_ANK9_499-528 aa
ANKHD1_ANK9_470-499 aa
EHMT2_ANK2_774-803 aa
EHMT1_ANK2_805-836 aa
ANKRD17_ANK20_1217-1246 aa
ANKHD1_ANK20_1189-1218 aa
ANKRD17_ANK17_1115-1144 aa
ANKHD1_ANK17_1087-1116 aa
ANKRD17_ANK24_1352-1381 aa
ANKHD1_ANK24_1324-1353 aa
ANKRD17_ANK14_663-692 aa
ANKHD1_ANK14_634-663 aa
ANKRD17_ANK21_1251-1280 aa
ANKHD1_ANK21_1223-1252 aa
ANKRD17_ANK18_1149-1178 aa
ANKHD1_ANK18_1121-1150 aa
ANKRD17_ANK16_1082-1111 aa
ANKHD1_ANK16_1054-1083 aa
CDKN2C_ANK4_136-167 aa
ANKRD17_ANK4_333-362 aa
ANKHD1_ANK4_304-333 aa
ANKRD17_ANK12_596-625 aa
ANKHD1_ANK12_567-596 aa
ANKRD17_ANK10_533-562 aa
ANKHD1_ANK10_504-533 aa
ANKRD17_ANK6_400-429 aa
ANKHD1_ANK6_371-400 aa
ANKRD17_ANK8_466-495 aa
ANKHD1_ANK8_437-466 aa
ANKRD17_ANK23_319-1348 aa
ANKHD1_ANK23_1291-1320 aa
ANKRD17_ANK3_300-329 aa
ANKHD1_ANK3_271-300 aa
RFXANK_ANK2_134-163 aa
FEM1A_ANK3_82-111 aa
PPP1R12B_ANK1_56-86 aa
ANKRD17_ANK1_233-262 aa
ANKHD1_ANK1_204-233 aa
RFXANK_ANK1_101-130 aa
EHMT2_ANK4_841-870 aa
EHMT1_ANK4_872-901 aa
RFXANK_ANK3_167-196 aa
CLPB_ANK1_133-162 aa
KANK1_ANK4_1233-1262 aa
KANK1_ANK3_1195-1228 aa
ANKFY1_ANK17_947-976 aa
ACAP2_ANK1_640-669 aa
EHMT2_ANK1_741-770 aa
EHMT1_ANK1_772-801 aa
ANKRD17_ANK19_1182-1211 aa
ANKHD1_ANK19_1154-1183 aa
RFXANK_ANK4_200-229 aa
ANKFY1_ANK8_630-659 aa
CDKN2D_ANK1_41-69 aa
CDKN2C_ANK1_37-65 aa
ANKFY1_ANK15_878-907 aa
EHMT2_ANK6_907-936 aa
EHMT1_ANK6_938-967 aa
ACAP2_ANK2_673-702 aa
ANKRD11_ANK3_233-262 aa
ANKRD12_ANK3_250-279 aa
ANKFY1_ANK13_811-840 aa
PPP1R12C_ANK4_259-288 aa
PPP1R12B_ANK5_249-278 aa
FEM1A_ANK9_580-609 aa
ANKFY1_ANK18_980-1009 aa
ANKFY1_ANK7_584-614 aa
ANKFY1_ANK4_408-438 aa
ANKFY1_ANK14_844-872 aa
CDKN2C_ANK3_102-132 aa
CDKN2D_ANK3_106-134 aa
OSTF1_ANK2_105-135 aa
ANKRD17_ANK15_696-725 aa
ANKHD1_ANK15_667-696 aa
FEM1A_ANK2_40-70 aa
ANKRD17_ANK25_1385-1414 aa
ANKHD1_ANK25_1357-1390 aa
FEM1A_ANK4_115-145 aa
FEM1A_ANK7_214-243 aa
0. 1

Figure S2

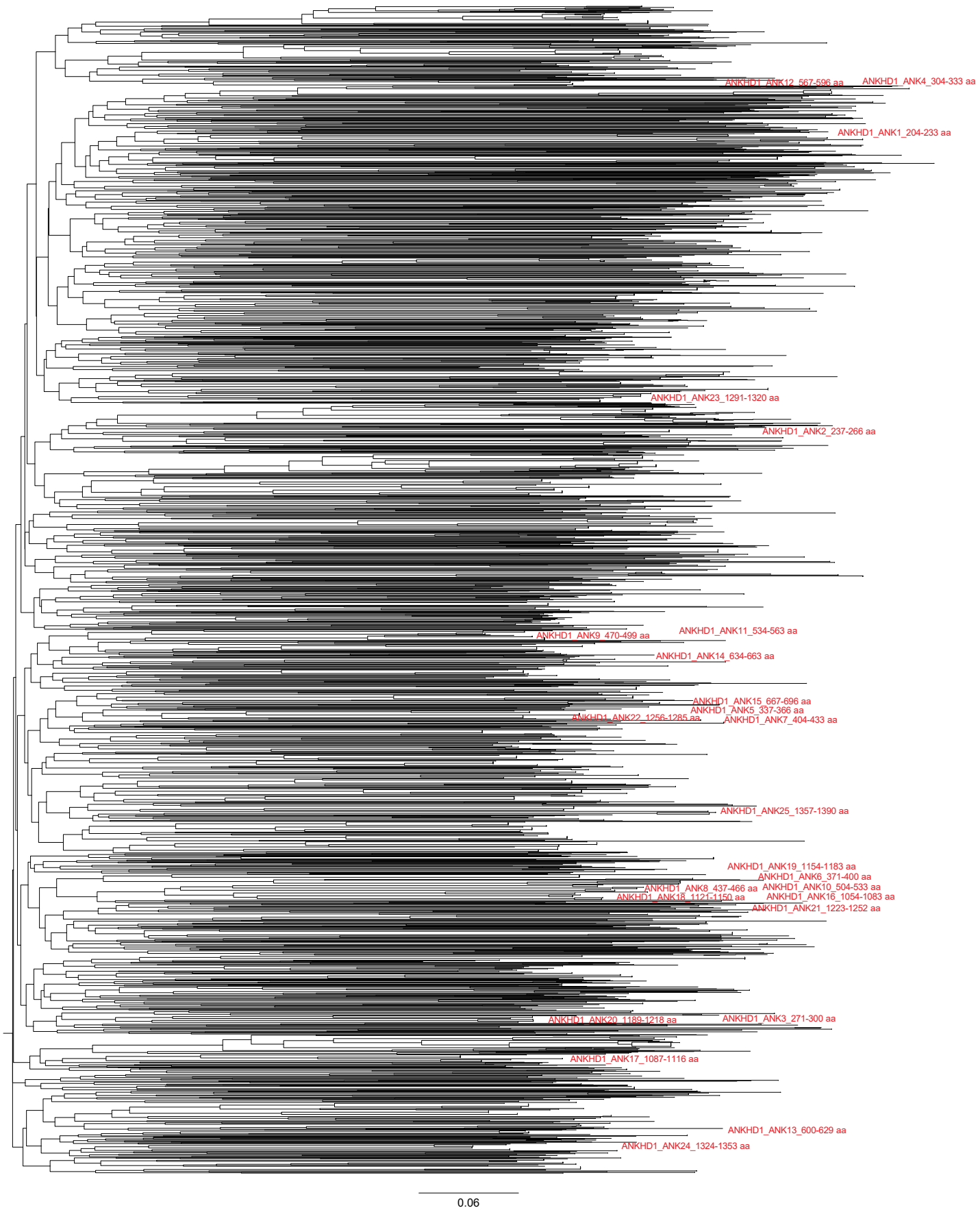
ANKHD1_ANK12_567-596 aa
ANKHD1_ANK4_304-333 aa
ANKHD1_ANK1_204-233 aa
ANKHD1_ANK23_1291-1320 aa
ANKHD1_ANK2_237-266 aa
ANKHD1_ANK9_470-499 aa
ANKHD1_ANK11_534-563 aa
ANKHD1_ANK14_634-663 aa
ANKHD1_ANK15_667-696 aa
ANKHD1_ANK5_337-366 aa
ANKHD1_ANK22_1256-1285 aa
ANKHD1_ANK7_404-433 aa
ANKHD1_ANK25_1357-1390 aa
ANKHD1_ANK19_1154-1183 aa
ANKHD1_ANK6_371-400 aa
ANKHD1_ANK8_437-466 aa
ANKHD1_ANK10_504-533 aa
ANKHD1_ANK18_1121-1150 aa
ANKHD1_ANK16_1054-1083 aa
ANKHD1_ANK21_1223-1252 aa
ANKHD1_ANK20_1189-1218 aa
ANKHD1_ANK3_271-300 aa
ANKHD1_ANK17_1087-1116 aa
ANKHD1_ANK13_600-629 aa
ANKHD1_ANK24_1324-1353 aa
0.06

Figure S3

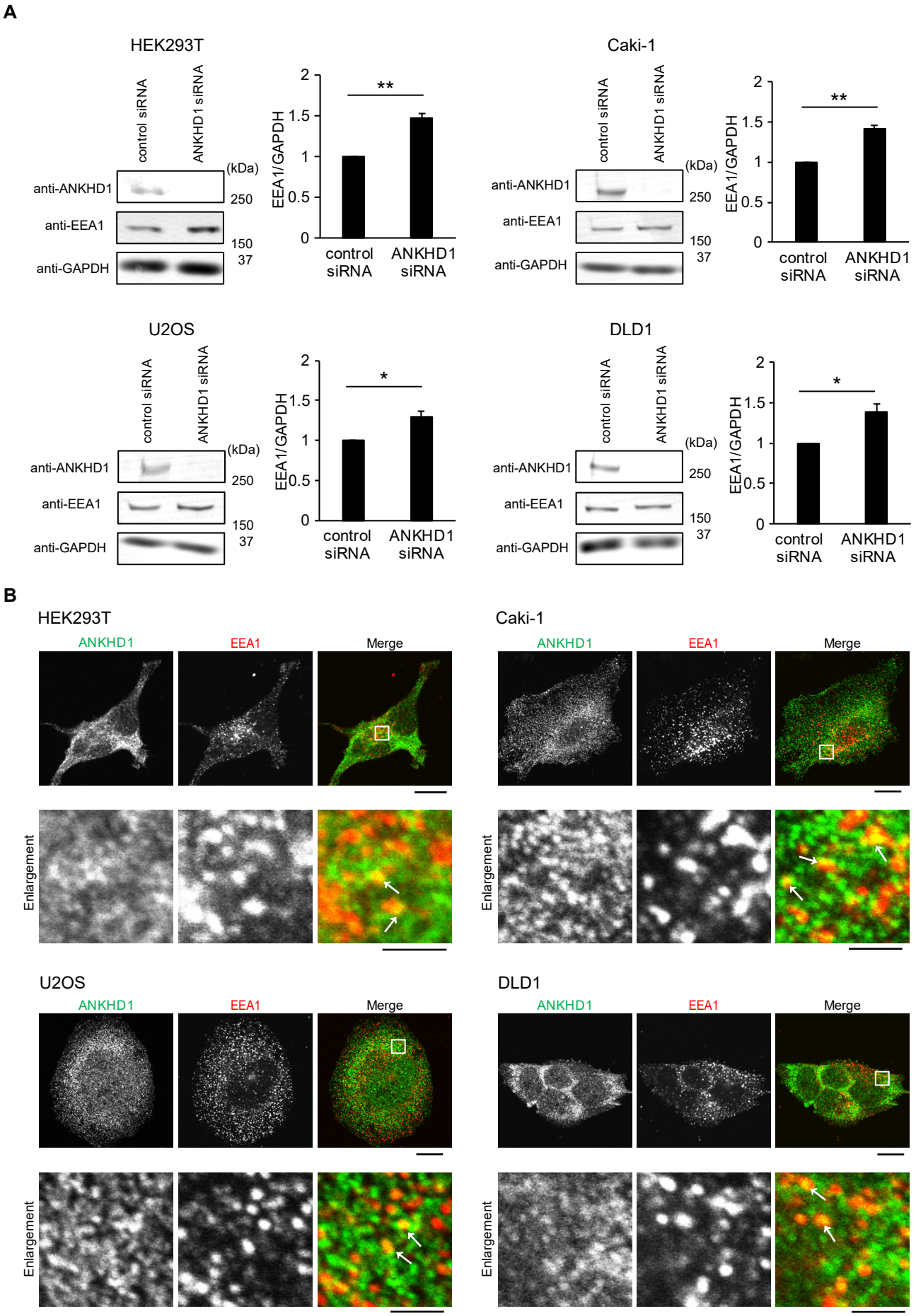
A
HEK293T
control siRNA
ANKHD1 siRNA
(kDa)
anti-ANKHD1
anti-EEA1
anti-GAPDH
250
150
37
EEA1/GAPDH
**
control siRNA
ANKHD1 siRNA
Caki-1
U2OS
*
DLD1
B
ANKHD1
EEA1
Merge
Enlargement

Figure S4

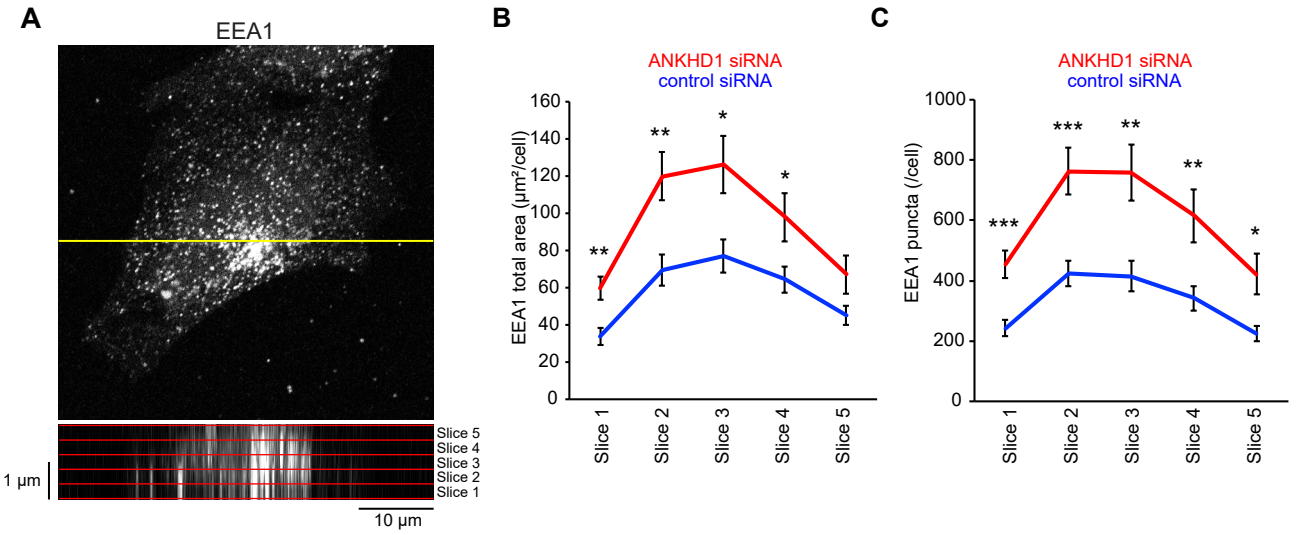
A
EEA1
Slice 5
Slice 4
Slice 3
Slice 2
Slice 1
1 μm
10 μm
B
ANKHD1 siRNA
control siRNA
EEA1 total area (μm²/cell)
160
140
120
100
80
60
40
20
0
**
**
*
*
Slice 1
Slice 2
Slice 3
Slice 4
Slice 5
C
ANKHD1 siRNA
control siRNA
EEA1 puncta (/cell)
1000
800
600
400
200
0
***
***
**
**
*
Slice 1
Slice 2
Slice 3
Slice 4
Slice 5

Figure S5

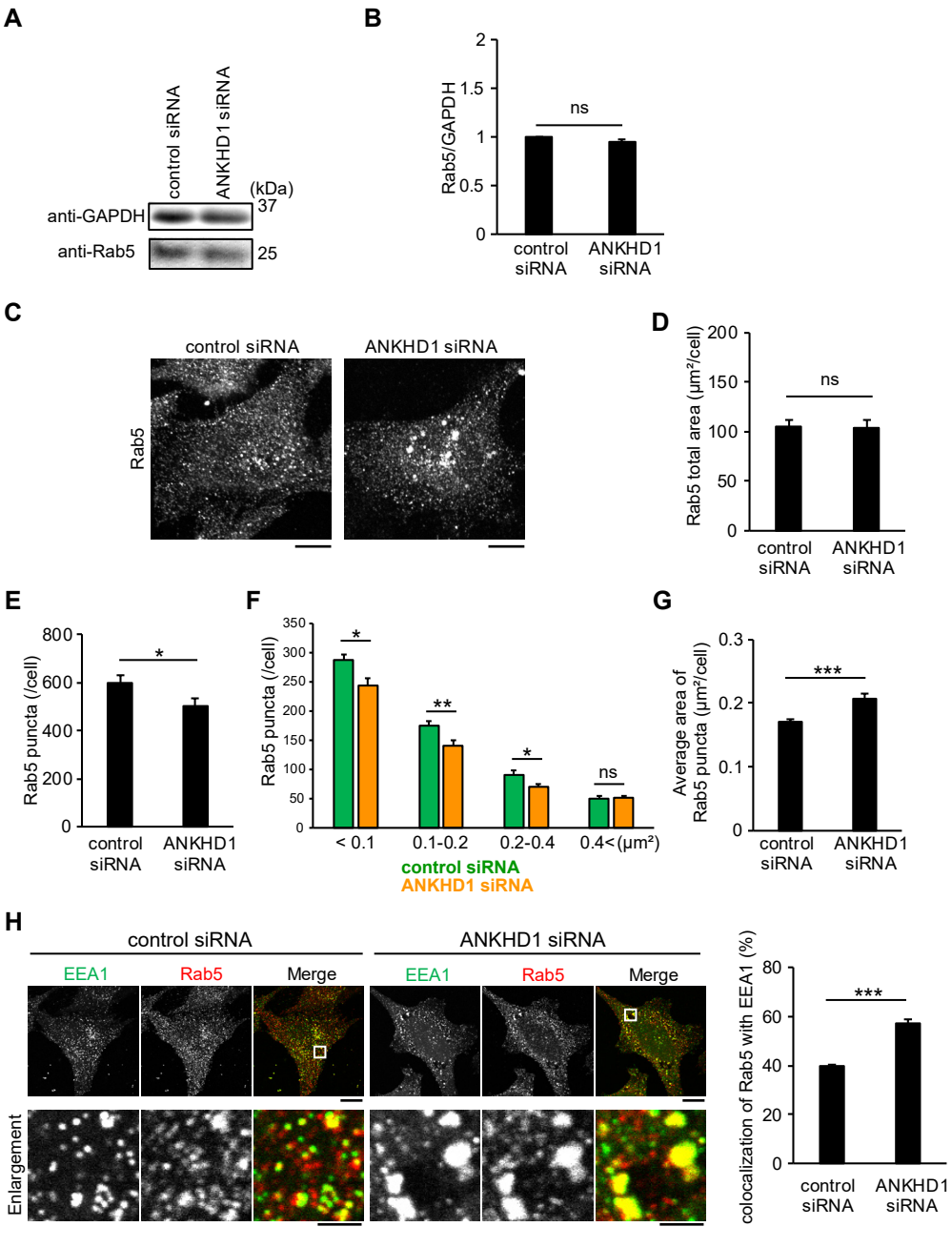
A
control siRNA
ANKHD1 siRNA
(kDa)
anti-GAPDH
37
anti-Rab5
25
B
Rab5/GAPDH
ns
control siRNA
ANKHD1 siRNA
C
control siRNA
ANKHD1 siRNA
Rab5
D
Rab5 total area (μm²/cell)
ns
E
Rab5 puncta (/cell)
F
Rab5 puncta (/cell)
< 0.1
0.1-0.2
0.2-0.4
0.4<(μm²)
control siRNA
ANKHD1 siRNA
G
Average area of Rab5 puncta (μm²/cell)
H
EEA1
Rab5
Merge
Enlargement
colocalization of Rab5 with EEA1 (%)

Figure S6

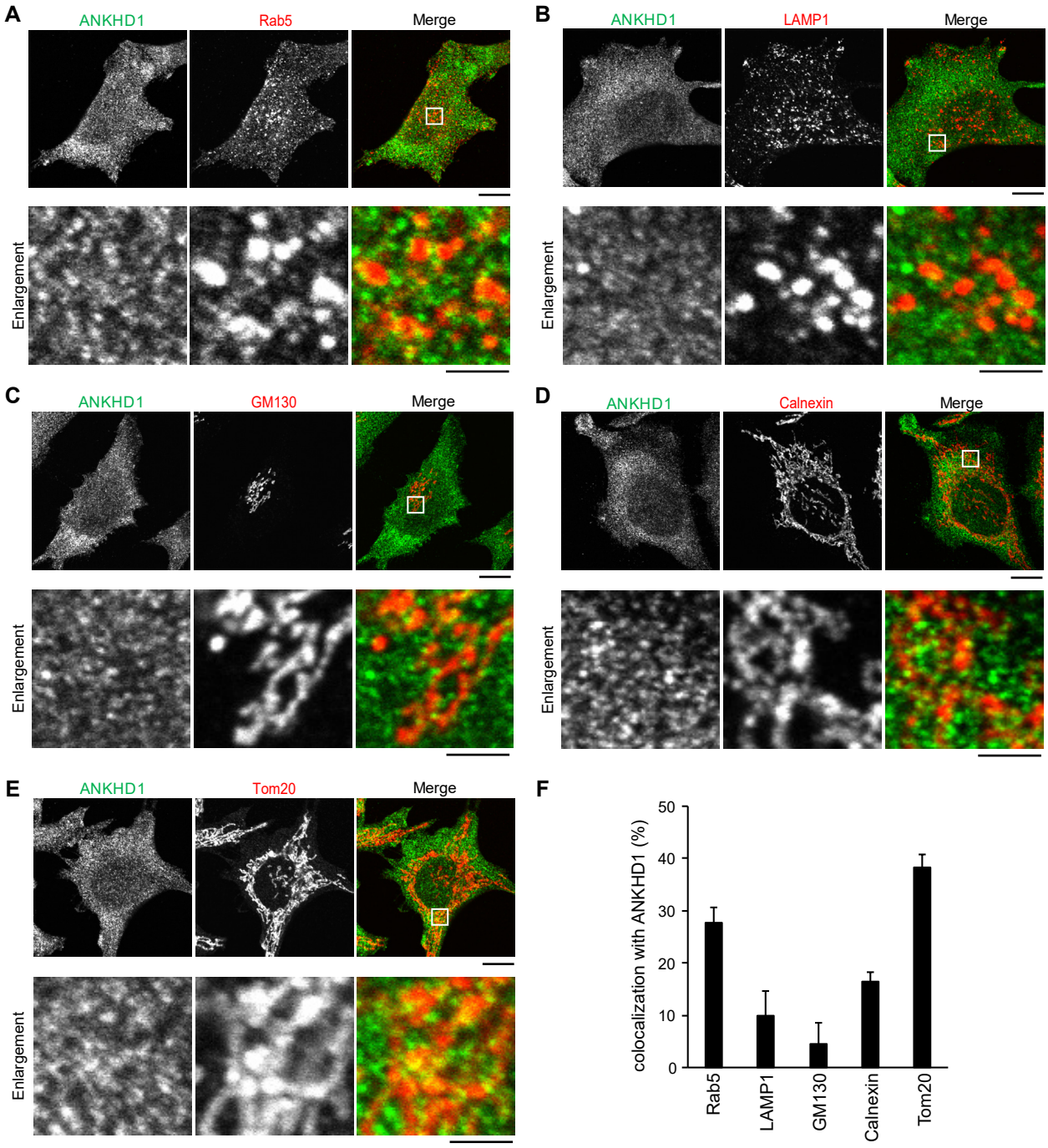
A
ANKHD1
Rab5
Merge
Enlargement
B
ANKHD1
LAMP1
Merge
Enlargement
C
ANKHD1
GM130
Merge
Enlargement
D
ANKHD1
Calnexin
Merge
Enlargement
E
ANKHD1
Tom20
Merge
Enlargement
F
colocalization with ANKHD1 (%)
50
40
30
20
10
0
Rab5
LAMP1
GM130
Calnexin
Tom20

Figure S7

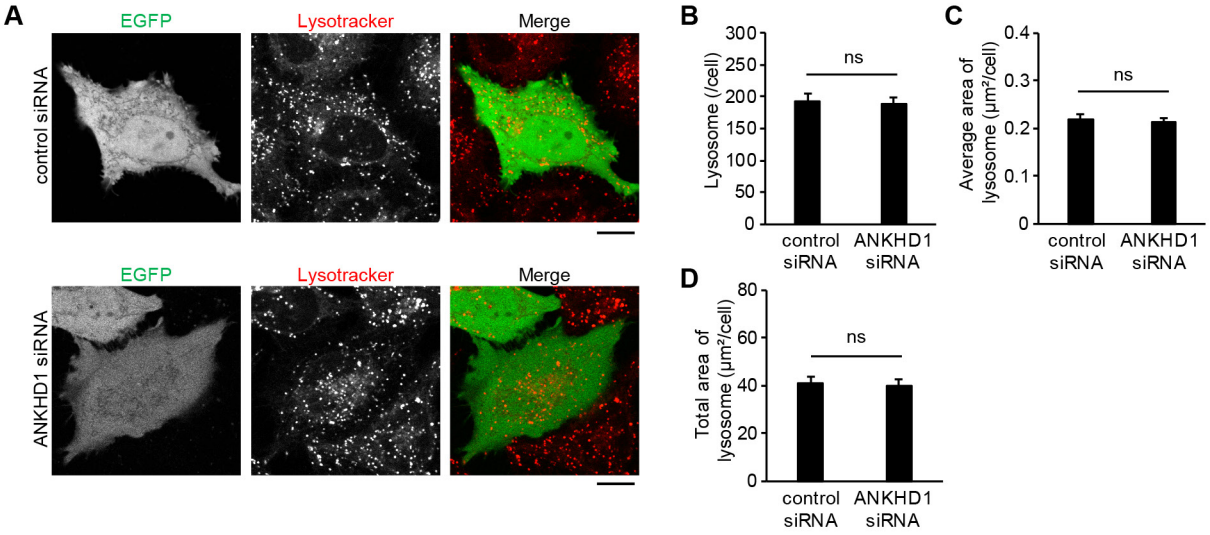
A
EGFP
Lysotracker
Merge
control siRNA
EGFP
Lysotracker
Merge
ANKHD1 siRNA
B
Lysosome (/cell)
300
250
200
150
100
50
0
ns
control siRNA
ANKHD1 siRNA
C
Average area of lysosome (μm²/cell)
0.4
0.3
0.2
0.1
0
ns
control siRNA
ANKHD1 siRNA
D
Total area of lysosome (μm²/cell)
80
60
40
20
0
ns
control siRNA
ANKHD1 siRNA

Figure S8

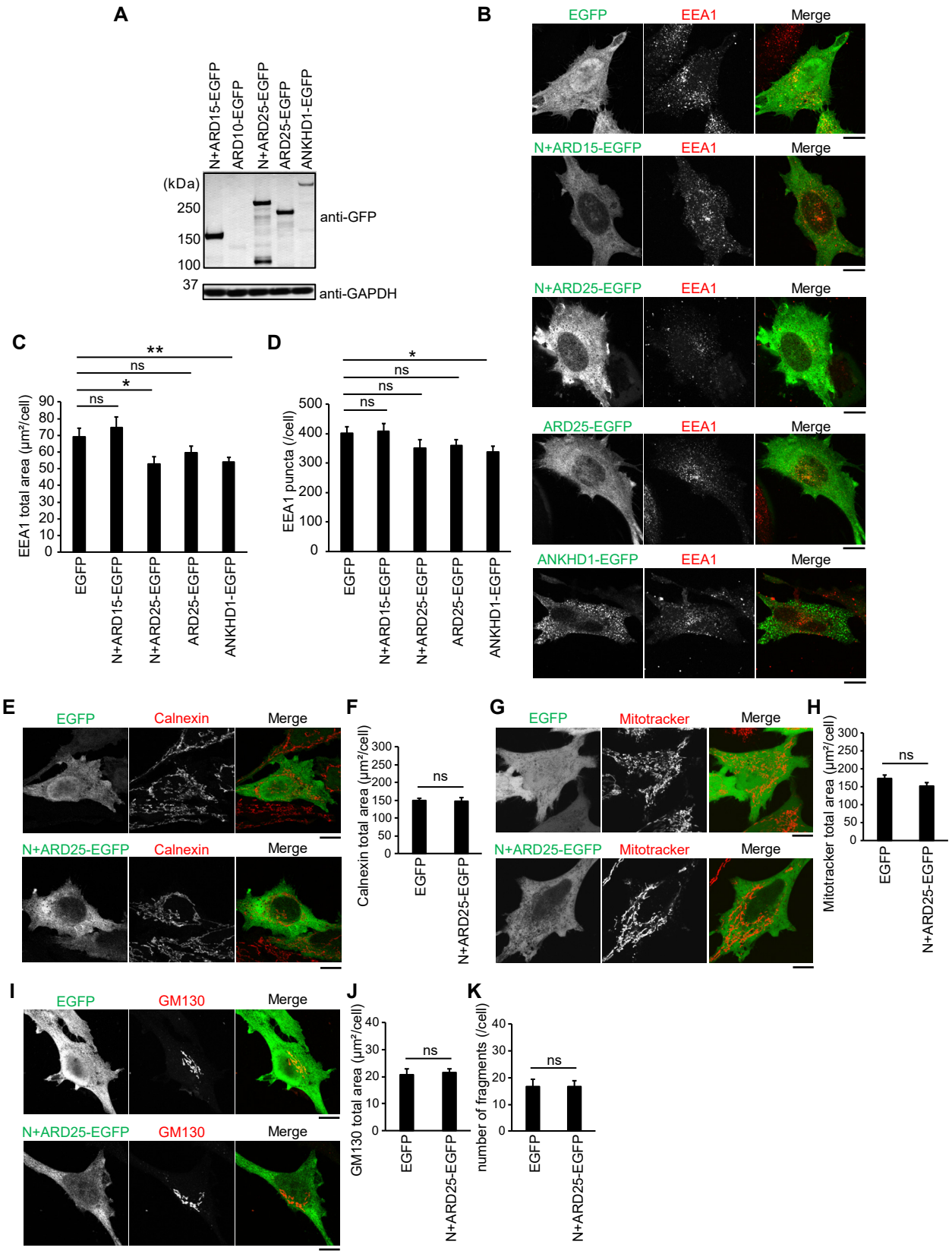
A
N+ARD15-EGFP
ARD10-EGFP
N+ARD25-EGFP
ARD25-EGFP
ANKHD1-EGFP
(kDa)
250
150
100
37
anti-GFP
anti-GAPDH
B
EGFP
EEA1
Merge
N+ARD15-EGFP
N+ARD25-EGFP
ARD25-EGFP
ANKHD1-EGFP
C
EEA1 total area (μm²/cell)
ns
*
**
D
EEA1 puncta (/cell)
E
Calnexin
F
Calnexin total area (μm²/cell)
G
Mitotracker
H
Mitotracker total area (μm²/cell)
I
GM130
J
GM130 total area (μm²/cell)
K
number of fragments (/cell)

Figure S9

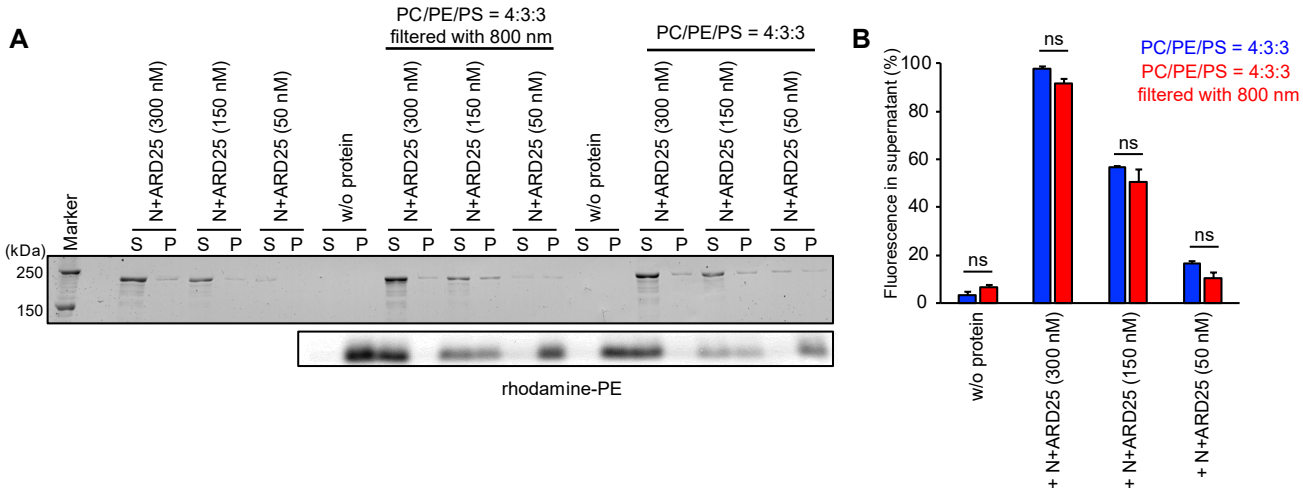
A
PC/PE/PS = 4:3:3
filtered with 800 nm
PC/PE/PS = 4:3:3
Marker
N+ARD25 (300 nM)
N+ARD25 (150 nM)
N+ARD25 (50 nM)
w/o protein
(kDa)
250
150
S P
rhodamine-PE
B
PC/PE/PS = 4:3:3
PC/PE/PS = 4:3:3
filtered with 800 nm
Fluorescence in supernatant (%)
100
80
60
40
20
0
ns
w/o protein
+ N+ARD25 (300 nM)
+ N+ARD25 (150 nM)
+ N+ARD25 (50 nM)

Figure S10

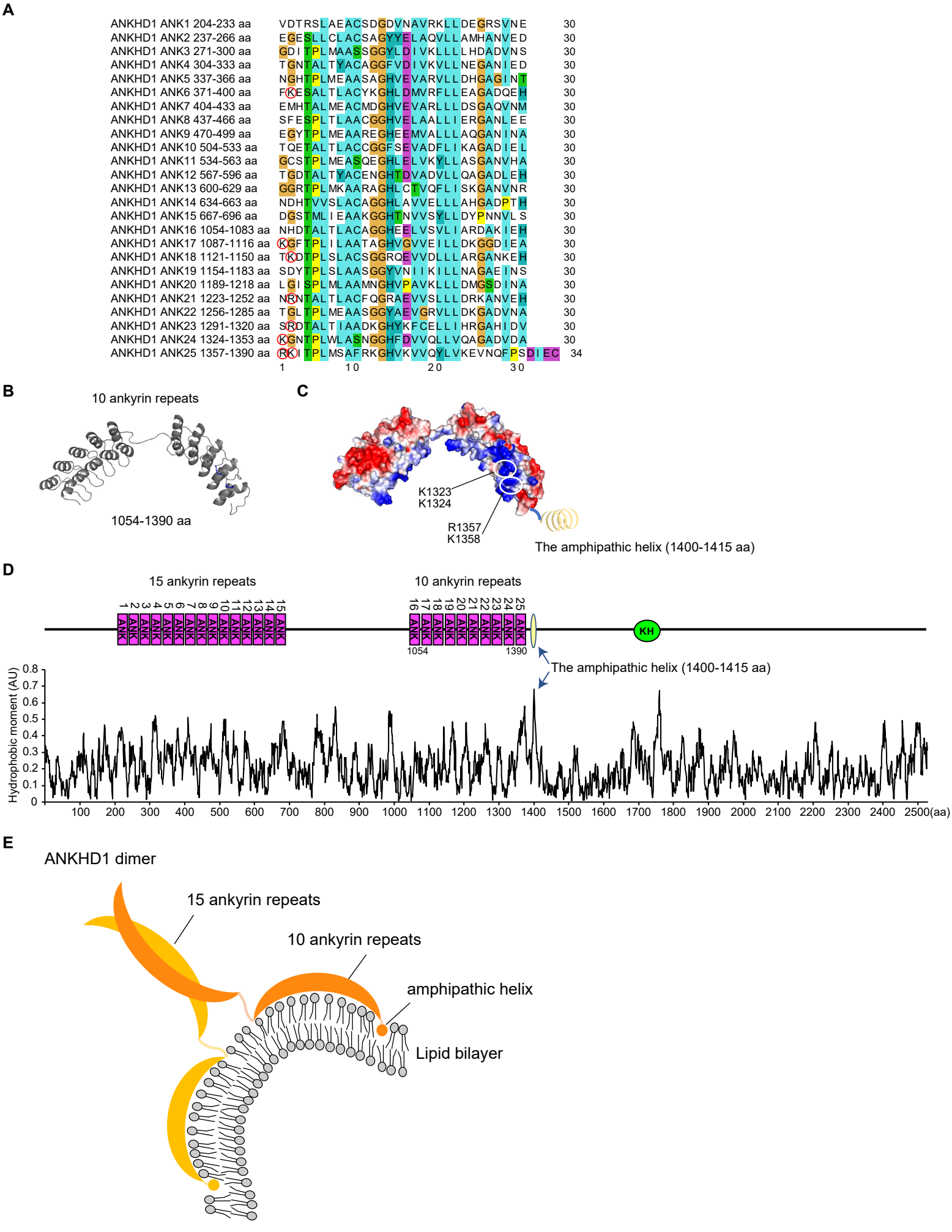
A
ANKHD1 ANK1 204-233 aa VDTRSLAEACSDGDVNAVRKLLDEGRSVNE 30
ANKHD1 ANK2 237-266 aa EGESLLCLACSAGYYELAQVLLAMHANVED 30
ANKHD1 ANK3 271-300 aa GDITPLMAASSGGYLDIVKLLLLHDADVNS 30
ANKHD1 ANK4 304-333 aa TGNTALTYACAGGFVDIVKVLLNEGANIED 30
ANKHD1 ANK5 337-366 aa NGHTPLMEAASAGHVEVARVLLDHGAGINT 30
ANKHD1 ANK6 371-400 aa FKESALTLACYKGHLDMVRFLLEAGADQEH 30
ANKHD1 ANK7 404-433 aa EMHTALMEACMDGHVEVARLLLDSGAQVNM 30
ANKHD1 ANK8 437-466 aa SFESPLTLAACGGHVELAALLIERGANLEE 30
ANKHD1 ANK9 470-499 aa EGYTPLMEAAREGHEEMVALLLAQGANINA 30
ANKHD1 ANK10 504-533 aa TQETALTLACCGGFSEVADFLIKAGADIEL 30
ANKHD1 ANK11 534-563 aa GCSTPLMEASQEGHLELVKYLLASGANVHA 30
ANKHD1 ANK12 567-596 aa TGDTALTYACENGHTDVADVLLQAGADLEH 30
ANKHD1 ANK13 600-629 aa GGRTPLMKAARAGHLCTVQFLISKGANVNR 30
ANKHD1 ANK14 634-663 aa NDHTVVSLACAGGHLAVVELLLAHGADPTH 30
ANKHD1 ANK15 667-696 aa DGSTMLIEAAKGGHTNVVSYLLDYPNNVLS 30
ANKHD1 ANK16 1054-1083 aa NHDTALTLACAGGHEELVSVLIARDAKIEH 30
ANKHD1 ANK17 1087-1116 aa KGFTPLILAATAGHVGVVEILLDKGGDIEA 30
ANKHD1 ANK18 1121-1150 aa TKDTPLSLACSGGRQEVVDLLLARGANKEH 30
ANKHD1 ANK19 1154-1183 aa SDYTPLSLAASGGYVNIIKILLNAGAEINS 30
ANKHD1 ANK20 1189-1218 aa LGISPLMLAAMNGHVPAVKLLLDMGSDINA 30
ANKHD1 ANK21 1223-1252 aa NRNTALTLACFQGRAEVVSLLLDRKANVEH 30
ANKHD1 ANK22 1256-1285 aa TGLTPLMEAASGGYAEVGRVLLDKGADVNA 30
ANKHD1 ANK23 1291-1320 aa SRDTALTIAADKGHYKFCELLIHRGAHIDV 30
ANKHD1 ANK24 1324-1353 aa KGNTPLWLASNGGHFDVVQLLVQAGADVDA 30
ANKHD1 ANK25 1357-1390 aa RKITPLMSAFRKGHVKVVQYLVKEVNQFPSDIEC 34
1 10 20 30
B
10 ankyrin repeats
1054-1390 aa
C
K1323
K1324
R1357
K1358
The amphipathic helix (1400-1415 aa)
D
15 ankyrin repeats
10 ankyrin repeats
ANK
KH
1054
1390
The amphipathic helix (1400-1415 aa)
Hydrophobic moment (AU)
0
0.1
0.2
0.3
0.4
0.5
0.6
0.7
0.8
100 200 300 400 500 600 700 800 900 1000 1100 1200 1300 1400 1500 1600 1700 1800 1900 2000 2100 2200 2300 2400 2500(aa)
E
ANKHD1 dimer
15 ankyrin repeats
10 ankyrin repeats
amphipathic helix
Lipid bilayer

Figure S11